

## Resonant Raman scattering from ZnTe microcrystals: Evidence for quantum size effects

S. Hayashi, H. Sanda, M. Agata, and K. Yamamoto

*Department of Electronic Engineering, Faculty of Engineering, Kobe University, Rokkodai-cho,  
Nada-ku, Kobe 657, Japan*

(Received 24 April 1989)

The size dependence of the resonant Raman scattering from gas-evaporated ZnTe microcrystals has been investigated. Under the 5145-Å excitation at 80 K, we found that as the size decreases the relative intensity of the 2LO line decreases, while that of the 1LO line increases. This can be well explained by the change in the resonance condition caused by the blue shift of the exciton ground-state energy. The observed temperature dependence of the intensities also supports the blue shift. A semiquantitative treatment of the intensities allowed us to obtain the size dependence of the exciton energy, which is in good agreement with recent results of a variational calculation.

### I. INTRODUCTION

Quantum size effects on electron-hole systems confined in semiconductor microcrystals have recently been a subject of intensive experimental and theoretical studies. Various types of microcrystalline samples such as colloidal particles,<sup>1,2</sup> gas-evaporated particles,<sup>3</sup> and particles embedded in solid matrices (glasses or crystals),<sup>4-7</sup> have been prepared, and their absorption and luminescence spectra have been measured. The effects of the three-dimensional confinement normally result in observable high-energy shifts of the absorption and luminescence peaks, which are in good agreement at least qualitatively with theoretical results.<sup>8-10</sup> In addition to the absorption and luminescence measurements, the measurement of the resonant Raman scattering is expected to be effective for the study of the quantum size effects, since the resonant intermediate states in semiconductors are usually exciton states and the resonant behavior of Raman lines will be very sensitive to changes in the exciton states. An attempt to observe the quantum size effects by Raman spectroscopy has been made by Papavasiliou,<sup>11</sup> who has measured the luminescence and Raman spectra of CdS small particles prepared by various methods. Rosseti, Nakahara, and Brus<sup>12</sup> also have reported Raman spectra of colloidal CdS particles. Although these authors claim to have observed the quantum size effects, their experiments have been limited to a few fixed sizes. No systematic size dependence of the resonant Raman spectra has been reported so far.

We have chosen the gas-evaporation technique to produce ZnTe microcrystals. As has been demonstrated for GaP microcrystals,<sup>13,14</sup> the technique allows us to easily vary the size and prepare samples suited for both Raman spectroscopy and electron microscopy. We were able to prepare ZnTe microcrystals ranging from 200 to 900 Å in average size. Since the Bohr radius of the exciton in ZnTe is relatively large ( $\sim 70$  Å), the size of the microcrystals produced enters in the range where the quantum size effects are observable.<sup>10</sup> In this paper we report results of a systematic measurement of the size dependence

of the resonant Raman scattering and demonstrate that the blue shift of the exciton ground-state energy can really be detected by Raman spectroscopy.

### II. EXPERIMENTAL DETAILS

ZnTe microcrystals were produced by evaporating polycrystalline ZnTe crystals from a tungsten basket in argon gas. Sootlike deposits were collected onto small pieces of Si wafer ( $5 \times 15 \times 0.5$  mm<sup>3</sup>) placed 5 cm above the heater. To obtain the particles of various sizes, the gas pressure and the heater temperature were varied. The samples were mounted on a sample holder of a conduction-type liquid-nitrogen cryostat, and the temperature was varied from 80 to 200 K with the aid of a temperature controller. The Raman spectra were recorded by a Spex Ramalog 5M spectrophotometer, equipped with a double monochromator and a photon-counting system. The 5145-Å line of an Ar-ion laser was used to excite the spectra. The laser beam was loosely focused on the sample surface by using a cylindrical lens, and the power was kept less than 1 mW to avoid the sample heating. The intensity of the 520-cm<sup>-1</sup> Raman line of the bare part of the Si substrate was used for the intensity calibration. After the Raman measurements, a part of the microcrystalline deposits were scraped off from the substrate and put on electron microscopic grids covered by thin carbon films. The grids were studied by a JEM-200CX electron microscope operated at 200 kV.

### III. RESULTS AND DISCUSSION

Transmission electron microscopy (TEM) images indicated that the relatively large ZnTe particles (larger than about 500 Å) are polyhedral, while smaller particles tend to be spherical. We determined the average size  $d$  directly from the TEM images. A detailed analysis of electron diffraction patterns revealed that the particles have the zinc-blende structure, but a small amount of the particles with the wurtzite structure are mixed. Although the wurtzite ZnTe particles were detected by the electron

diffraction, no feature attributable to the wurtzite particles was found in Raman spectra.

Figure 1 shows the size dependence of the Raman spectrum measured at 80 K. The sample with the average size  $d = 848 \text{ \AA}$  exhibits a series of  $n$ LO Raman lines up to  $n = 4$ ; among other lines, the 2LO line is the strongest. As the average size decreases, the absolute intensities of the lines rapidly decrease, and the 3LO and 4LO lines become too weak to be observed. The most important size effect seen in Fig. 1 is the change in the relative intensities of the 1LO and 2LO lines; as the size decreases, the 2LO line becomes weaker and weaker, while the 1LO line becomes stronger and stronger. In order to see more clearly this size dependence, the intensity ratio  $I_{2LO}/I_{1LO}$  is plotted in Fig. 2 as a function of the average particle size. We can see that the ratio increases almost linearly with the size. We note here that within the accuracy of the present measurement ( $\pm 1 \text{ cm}^{-1}$ ), no change in the LO phonon frequency ( $210 \text{ cm}^{-1}$ ) with decreasing the size was observed. In general, the Raman signal is quite sensitive to crystal orientation due to selection rules. However, results of our electron diffraction study showed no evidence for partial alignment of the microcrystals. We can thus exclude the orientation effect as the cause of the size dependence of the Raman spectrum described in the above.

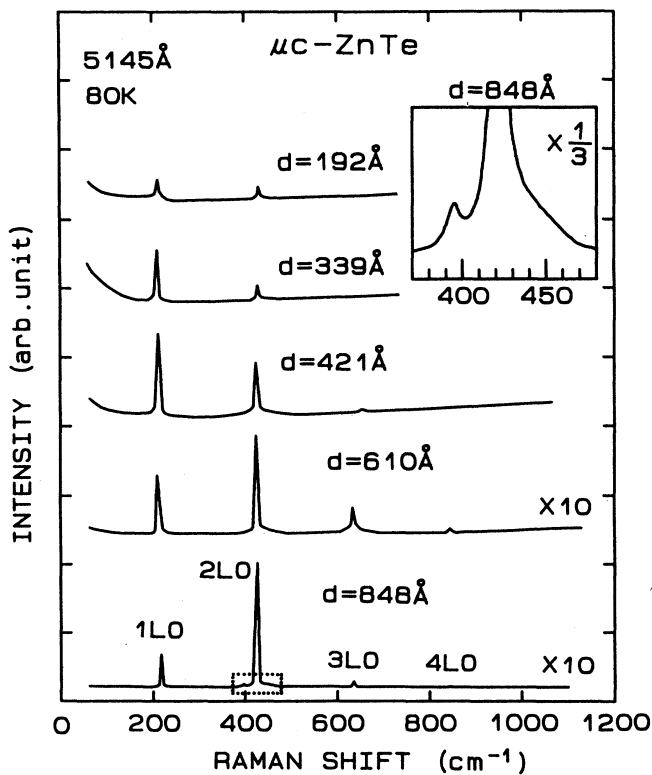


FIG. 1. Size dependence of resonant Raman scattering from gas-evaporated ZnTe microcrystals;  $d$  is the average particle size. In the inset a part of the spectrum for  $d = 848 \text{ \AA}$  near the 2LO line is enlarged.

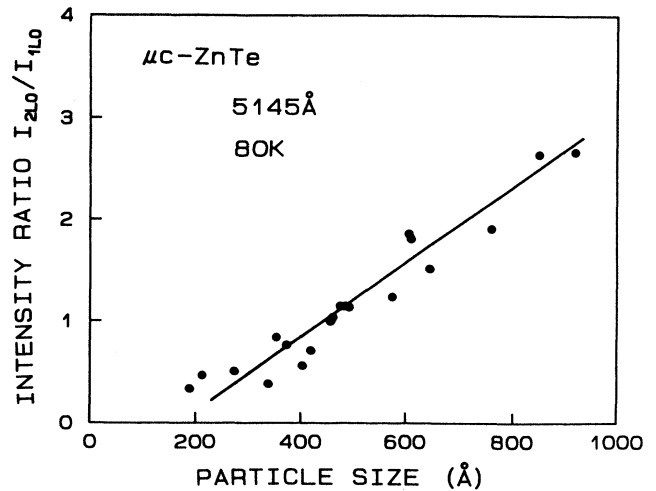


FIG. 2. Size dependence of the ratio of the 2LO intensity to the 1LO intensity. The solid line is only a guide to the eyes.

We now compare our results with data of bulk ZnTe crystals. According to Kwietniak, Oka, and Kushida,<sup>15</sup> bulk ZnTe crystals exhibit  $n$ LO lines as well as a free-exciton (FE) luminescence band in the temperature range between 77 and 170 K; at 77 K the FE band is located in between the 1LO and 2LO lines, and as the temperature increases, the band shifts to lower energies, passing through the 2LO line at about 95 K and the 3LO line at about 140 K (see Figs. 1 and 2 in Ref. 15). The intensities of the 2LO and 3LO lines take the maximum values when the FE band coincides in position with these lines. A close examination of the spectrum for the sample with  $d = 848 \text{ \AA}$  shown in Fig. 1 reveals that a very weak structure is visible around the 2LO line; the structure is enlarged and shown in the inset of this figure. This weak structure is attributable to the FE band, but its intensity is much smaller than that in bulk crystals. The FE band is too weak to be observed for smaller microcrystals. We believe that the rate of the nonradiative decay of excitons at surfaces is extremely high in our gas-evaporated microcrystals, thereby reducing very much the FE luminescence intensity. In contrast to the present result, the FE luminescence bands with measurable intensities have been observed for cuprous halide microcrystals embedded in alkali halide matrices.<sup>6,7</sup> The surfaces of microcrystals embedded in solid matrices are not free and fixed by the surrounding materials. In such microcrystals the nonradiative decay of excitons at surfaces seems to be less important than in the gas-evaporated microcrystals, which are nearly free standing and have free surfaces.

In bulk ZnTe crystals at around 80 K, the intensity of the 2LO line is resonantly enhanced, since the ground-state energy of the exciton is very near to the energy of the 2LO line.<sup>15</sup> Figure 1 demonstrates that the same holds for relatively large microcrystals. However, as the size decreases, the 2LO line is no more enhanced and the resonance moves to the 1LO line. The increase in the 1LO intensity and the decrease in the 2LO intensity can

be well explained by the change in the resonance condition caused by the blue shift of the exciton ground-state energy. In our ZnTe microcrystals about 200 Å in size, it is very likely that the exciton energy is blue shifted by approximately the LO-phonon energy (26 meV).

In order to confirm the above interpretation, we measured the temperature dependence of the Raman spectrum. In general the exciton energy decreases with increasing the temperature. Thus, the blue-shifted exciton energy in small enough microcrystals should shift back to lower energies and the relative intensities of the  $n$ LO lines should change. The changes in the relative intensities can really be observed as shown in Fig. 3, in which the temperature dependence of the Raman spectrum measured for a sample with  $d = 274$  Å is shown. As the temperature increases from 90 to 170 K, the absolute intensities of the 1LO, 2LO, and 3LO lines decrease rapidly and simultaneously the intensities of the 2LO and 3LO lines relative to that of the 1LO change appreciably. In order to see more clearly this change, the intensity ratios,  $I_{2LO}/I_{1LO}$  and  $I_{3LO}/I_{1LO}$ , measured in a 10-K step are plotted in Fig. 4. We can clearly see that as the temperature increases, the relative intensity of the 2LO line first increases, reaches a maximum at about 130 K, and then decreases, while that of the 3LO line first increases and reaches a maximum at around 170 K. These changes in the relative intensities can be well explained by the red shift of the exciton energy caused by the temperature rise, thereby confirming the initial blue shift at lower

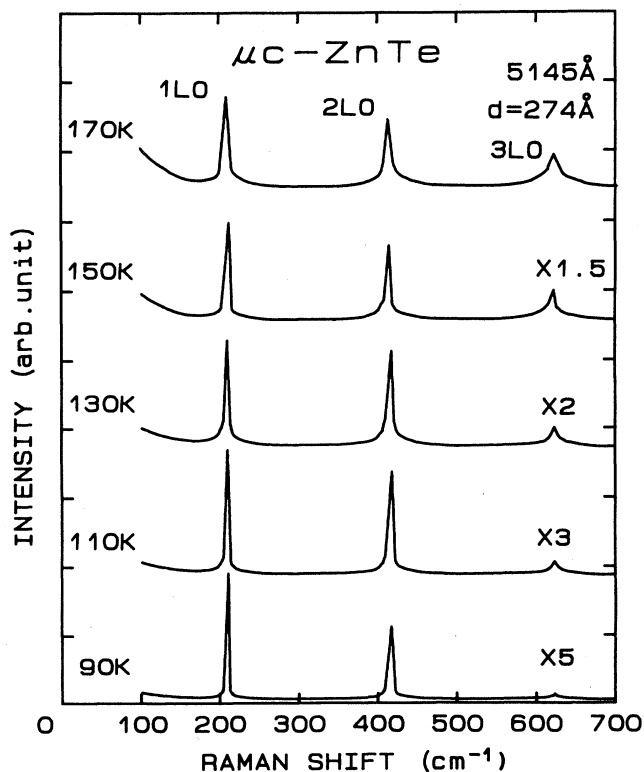


FIG. 3. Temperature dependence of resonant Raman scattering measured for a sample with  $d = 274$  Å.

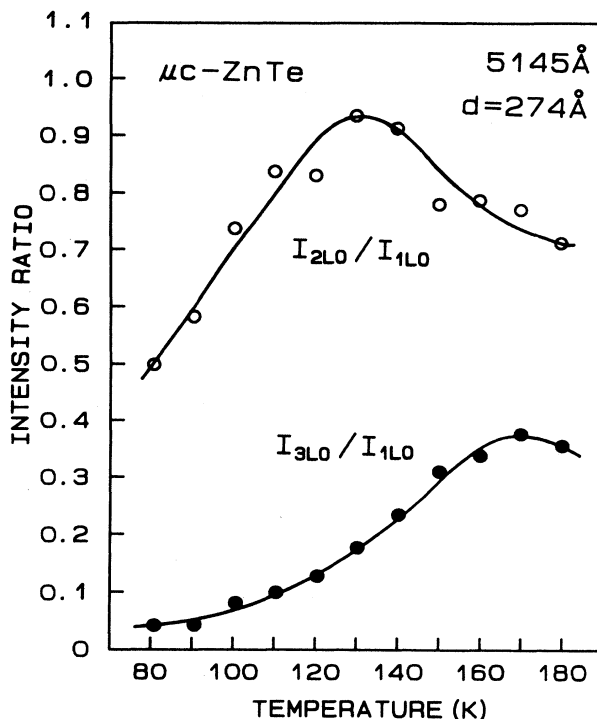


FIG. 4. Temperature dependence of the intensity ratios,  $I_{2LO}/I_{1LO}$  and  $I_{3LO}/I_{1LO}$ . The solid lines are only guides to the eyes.

temperatures. The exciton energy initially located around the 1LO line shifts to the energy of the 2LO line at about 130 K and to that of the 3LO line at about 170 K.

Kwietniak, Oka, and Kushida<sup>15</sup> have demonstrated that the resonant behavior of the 1LO and 2LO lines in bulk ZnTe can be well described by simple expressions of energy denominators in Raman tensors, which assume the ground state of exciton as the intermediate state. Using the same expressions of the denominators as used for bulk ZnTe [Eqs. (1) and (2) in Ref. 15], we tried to estimate the exciton energy in our microcrystals. Since the polariton effects and the correction for absorption coefficients are not taken into account in the present treatment, the estimation should be considered as semi-quantitative. Taking the ratio of the expressions for 1LO and 2LO intensities and solving for the exciton energy  $E_{ex}$ , we obtain

$$E_{ex} = E_i - 2E_{LO} + (C/A)^{1/2},$$

where  $E_i$  is the energy of the incident light (2.410 eV),  $E_{LO}$  is that of the LO phonon (26 meV),  $A$  is the ratio of the 2LO to the 1LO intensity, and  $C$  is a constant. Since the size dependence of the intensity ratio  $A$  has been measured (Fig. 2), that of  $E_{ex}$  can be obtained from the above equation provided that the constant  $C$  is known. To determine the value of  $C$  we assumed that in large enough microcrystals the exciton quantum size effects are negligibly small, and the exciton energy is the same as that of

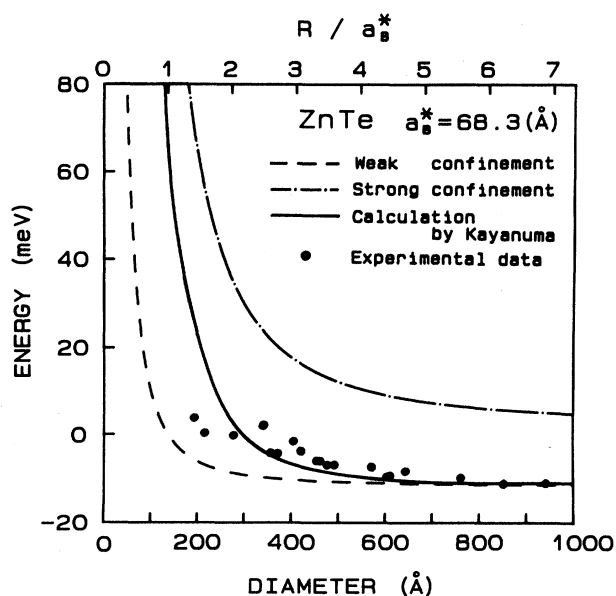


FIG. 5. Comparison of the experimental size dependence of exciton energy with theoretical results of Kayanuma (Ref. 10); the experimental size dependence was obtained from the intensity ratio shown in Fig. 2. The solid line represents the result of variational calculation. The dashed and dashed-dotted lines represent two limiting cases, weak and strong confinement, respectively. The zero of the ordinate corresponds to the bottom of the conduction band in bulk ZnTe.

the bulk crystal (2.366 eV at 80 K);<sup>15</sup> in practice, we used the value of  $A$  measured for a sample with  $d = 922$  Å.

The size dependence of  $E_{\text{ex}}$  obtained by the above method is plotted in Fig. 5 together with curves calculated from the theoretical results of Kayanuma.<sup>10</sup> In this figure the zero of the ordinate corresponds to the bottom of the conduction band in bulk crystals. The data points for large microcrystals ( $d > \sim 700$  Å) are located about 11 meV below the bottom of the conduction band; the binding energy of the exciton in bulk ZnTe is 11.6 meV.<sup>16</sup> As the size decreases, although the data points scatter to some extent, the exciton energy tends to increase; for  $d = \sim 200$  Å, the blue shift of the exciton energy amounts to 20 meV, which is comparable to the LO phonon ener-

gy. The solid line in the figure represents the result of variational calculation made by Kayanuma for the ground-state energy of the electron-hole system confined in a spherical quantum well; the result for  $\sigma = m_h/m_e = 5$  tabulated in Table I in Ref. 10 is plotted here, where  $m_e$  and  $m_h$  are electron and hole effective masses, respectively. The dashed line represents the limit of weak confinement (exciton confinement), while the dashed-dotted line represents the limit of strong confinement (individual particle confinement) (see Ref. 10 for detailed explanations). To convert the dimensionless quantities in Kayanuma's results into quantities appropriate for ZnTe, we used the following parameters:  $m_e = 0.09m_0$ ,  $m_h = 0.6m_0$ ,<sup>17</sup> and  $\epsilon = 10.1$ ,<sup>18</sup> where  $m_0$  is the electron mass in vacuum and  $\epsilon$  is the dielectric constant. We can see that the data points obtained from the present experiment are in good agreement with the result of the variational calculation as it should be, since the size of microcrystals studied enters in the intermediate region, where the size is so small that the picture of exciton confinement begins to fail and the size is too large for the picture of individual particle confinement to be valid.

#### IV. CONCLUSION

From a systematic measurement of the size dependence of resonant Raman scattering from gas-evaporated ZnTe microcrystals, we have demonstrated that the quantum size effects manifest themselves as the changes in the relative intensities of multiple LO phonon lines. The observed size dependence and temperature dependence of the relative intensities can be well explained by the blue shift of the exciton ground-state energy. A semiquantitative treatment of the intensities enabled us to deduce the size dependence of the exciton energy, which is in good agreement with the variational calculation of Kayanuma. Raman spectroscopy is extremely effective for the study of quantum size effects in gas-evaporated microcrystals, for which the exciton luminescence band is too weak to be observed presumably due to the increased nonradiative decay of excitons at surfaces.

#### ACKNOWLEDGMENTS

This work was supported by a Grant-in-Aid for Scientific Research on Priority Areas from the Ministry of Education, Science and Culture, Japan.

<sup>1</sup>R. Rossetti, J. L. Ellison, J. M. Gibson, and L. E. Brus, *J. Chem. Phys.* **80**, 4464 (1984).  
<sup>2</sup>C. J. Sandroff, D. M. Hwang, and W. M. Chung, *Phys. Rev. B* **33**, 5953 (1986).  
<sup>3</sup>S. Hayashi and K. Yamamoto, *J. Phys. Soc. Jpn.* **56**, 2229 (1987).  
<sup>4</sup>A. I. Ekimov, A. L. Éfros, and A. A. Onuschchenko, *Solid State Commun.* **56**, 921 (1985).  
<sup>5</sup>J. Warnock and D. D. Awschalom, *Phys. Rev. B* **32**, 5529 (1985).  
<sup>6</sup>T. Itoh, Y. Iwabuchi, and M. Kataoka, *Phys. Status Solidi B*

**145**, 567 (1988).  
<sup>7</sup>T. Itoh, Y. Iwabuchi, and T. Kirihara, *Phys. Status Solidi B* **146**, 531 (1988).  
<sup>8</sup>A. L. Éfros and A. L. Éfros, *Fiz. Tekh. Poluprovodn.* **16**, 497 (1982) [*Sov. Phys.—Semicond.* **16**, 772 (1982)].  
<sup>9</sup>L. E. Brus, *J. Chem. Phys.* **80**, 4403 (1984).  
<sup>10</sup>Y. Kayanuma, *Phys. Rev. B* **38**, 9797 (1988).  
<sup>11</sup>G. C. Papavassiliou, *J. Solid State Chem.* **40**, 330 (1981).  
<sup>12</sup>R. Rossetti, S. Nakahara, and L. E. Brus, *J. Chem. Phys.* **79**, 1086 (1983).  
<sup>13</sup>S. Hayashi and H. Kanamori, *Phys. Rev. B* **26**, 7079 (1982).

- <sup>14</sup>S. Hayashi, R. Koh, Y. Ichiyama, and K. Yamamoto, Phys. Rev. Lett. **60**, 1085 (1988).
- <sup>15</sup>M. Kwietniak, Y. Oka, and T. Kushida, J. Phys. Soc. Jpn. **44**, 558 (1978).
- <sup>16</sup>T. Taguchi, S. Fujita, and Y. Inuishi, J. Cryst. Growth **45**, 304 (1978).
- <sup>17</sup>R. E. Nahory and H. Y. Fan, Phys. Rev. Lett. **17**, 251 (1966).
- <sup>18</sup>D. A. Berlincourt, H. Jaffe, and L. R. Shiozawa, Phys. Rev. **129**, 1009 (1963).